Available online at www.sciencedirect.com
ScienceDirect
Acta Biomaterialia 2 (2006) 493–504
Acta BIOMATERIALIA
www.actamat-journals.com

Stresses in growing soft tissues

K.Y. Volokh *,[1]

Department of Mechanical Engineering, Johns Hopkins University, Baltimore, MD, United States

Received 21 December 2005; received in revised form 5 April 2006; accepted 17 April 2006

Abstract

Biochemical processes of tissue growth lead to production of new proteins, cells, and other material particles at the microscopic level. At the macroscopic level, growth is marked by the change of the tissue shape and mass. In addition, the appearance of the new material particles is generally accompanied by deformation and, consequently, stresses in the surrounding material. Built upon a microscopic toy-tissue model mimicking the mechanical processes of mass supply, a simple phenomenological theory of tissue growth is used in the present work for explaining residual stresses in arteries and studying stresses around growing solid tumors/multicell spheroids. It is shown, in particular, that the uniform volumetric growth can lead to accumulation of residual stresses in arteries because of the material anisotropy. This can be a complementary source of residual stresses in arteries as compared to the stresses induced by non-uniform tissue growth. It is argued that the quantitative assessment of the residual stresses based on *in vitro* experiments may not be reliable because of the essential stress redistribution in the tissue samples under the cutting process. Concerning the problem of tumor growth, it is shown that the multicell spheroid or tumor evolution depends on elastic properties of surrounding tissues. In good qualitative agreement with the experimental *in vitro* observations on growing multicell spheroids, numerical simulations confirm that stiff hosting tissues can inhibit tumor growth.

Keywords: Growth; Soft tissue; Artery; Residual stresses; Tumor

1. Introduction

Understanding growth of living tissues is of fundamental theoretical and practical interest. Analytical models of growth of both plant and animal tissues can predict the evolution of the tissue, which may improve the treatment of pathological conditions and offer new prospects in tissue engineering. Biological or biochemical mechanisms of growth are not well understood although plenty of scenarios exist in the biological literature. There is no doubt that biochemistry is the driving force of tissue growth. Understanding the biochemistry of growth is most desirable. Biochemistry can explain why a tissue grows. This is not enough, however. It is also necessary to know how a tissue grows. The latter means macroscopic description in terms of the macroscopically measurable parameters. There is no shortage of macroscopic models of soft tissue growth [1–18]. However, the mathematical apparatus of the existing approaches is rather complicated and it includes variables that are difficult to interpret in simple terms and to assess in measurements, such as the cofactors in the multiplicative decomposition of the deformation gradient or the partial stresses and tractions in the mixture theories. This complexity requires an additional effort for the careful experimental calibration of the theories as, for example, in the case of the cartilage growth considerations by Klisch et al. [19,20].

In the present work, a continuum mechanics framework for modeling growth of living tissues is used, which does not include internal variables [21,22].[2] Moreover, this

* Tel.: +1 410 516 5134.
E-mail address: kvolokh@jhu.edu
[1] On leave of absence from the Technion – Israel Institute of Technology.

[2] Guillou and Ogden [23] present an alternative theory of soft tissue growth without the internal variables.

1742-7061/$ - see front matter © 2006 Acta Materialia Inc. Published by Elsevier Ltd. All rights reserved.
doi:10.1016/j.actbio.2006.04.002

theory is driven by a simple microstructural model of material supply that motivates the balance and constitutive equations. Two applications of the growth theory presented are considered.

First, the formation of residual stresses in arteries under the restriction of purely genetic and uniform mass supply is studied. It is shown that the arterial anisotropy can play the crucial role in the appearance and accumulation of stresses in growth. This is complementary to a more traditional point of view, which attributes residual stresses to non-uniform (differential) growth. We emphasize that the quantitative assessment of the residual stresses in arteries would require *in vivo* experiments. The existing *in vitro* experiments may lead to inaccurate estimates of residual stresses because of the necessity to cut the arterial pieces. The cutting process is accompanied by a redistribution of stresses, which can essentially affect their estimates. We propose a possible experiment in order to emphasize the stress redistribution issue in the *in vitro* tests.

Second, we apply the theory to the study of stresses around growing solid tumors. A growing tumor may press neighbor tissues and lead to their remodeling and necrosis or, ultimately, to the failure of organs to carry out their regular functions. For example, expanding tumors can initiate the collapse of immature blood vessels formed during the angiogenic phase, and the inflation and rupture of capsules, membranes and ducts the tumor grows into. Another example is an expanding brain tumor, which can deform brain areas responsible for various kinds of human activity and disturb the normal action of the organism. Thus, it can be important to know what is the expected tumor shape and mass for planning the date and strategy of operative invasion. A simplistic description of tumor development is attributed to Winsor [24], who adapted Gompertz's [25] empirical formula for modeling tumor growth: $\ln(\ln(V/V_0)) = -vt + V_{\max}/V_0$, where V is a measure of tumor size, V_0 the initial size, and $V_{\max}$ the final size. The rate of cell proliferation is v and t is time. Evidently, this formula accounts neither for tissue elasticity nor for material supply. However, recent experiments with tumor cell spheroids demonstrate the importance of these issues and the deficiency of the Gompertz simple formula. In particular, mimicking tumor development *in vivo*, Helmlinger et al. [26] considered *in vitro* growth of multicell tumor spheroids embedded in agarose gels. Spheroids were cultured in gels of increasing agarose concentration, thereby increasing the stiffness of the embedding matrix. It was observed that tumor growth was inhibited by the increasing gel stiffness. Evidently, this result emphasizes the role of the hosting tissue in the tumor growth process *in vivo*. Mathematical modeling of solid tumor growth has a long history [27]; however, the main emphasis of the research has been on problems of fluid transport and chemical reactions during the process of tumor formation [28–44]. Elasticity of the tumor/multicell spheroid was recently considered by Ambrosi and Mollica [45,46] who used a rather abstract approach, typical of the theories of soft tissue growth when the deformation gradient is decomposed into growth and elastic cofactors that correspond to the incompatible 'pure growth' of the material and the elastic deformation providing the final material compatibility. Contrary to Refs. [45,46] we will use a growth theory that does not introduce internal variables and that can be directly calibrated in experiments. We will show that stiff hosting tissues can inhibit tumor growth in a good qualitative agreement with the *in vitro* observations of growing multicell spheroids.

2. Methods

2.1. Governing equations

The assumption that continuous deformation and mass flow can describe the mechanics of growing living bodies is central to further development. To make this assumption sound, the geometry of growth should be analyzed qualitatively. A sharp distinction between the real physical material, i.e., material particles comprising continuum, and the mathematical concept of material point should be kept in mind. This distinction is illustrated in Fig. 1, where material deformation-growth is considered on different length scales. On the macroscopic scale, we assume that a material body can be divided into an infinite set of material points. It is assumed that position $\mathbf{X}$ in the physical space can be ascribed to every material point before growth-deformation. These material points form the material continuum. It is further assumed that during growth-deformation every point moves to a new position $\mathbf{x} = \boldsymbol{\chi}(\mathbf{X})$ preserving the compatibility of the body. This mapping is smooth to the necessary degree. Moreover, it is assumed that the mapping is one-to-one, i.e., the 'infinite number' of material points is

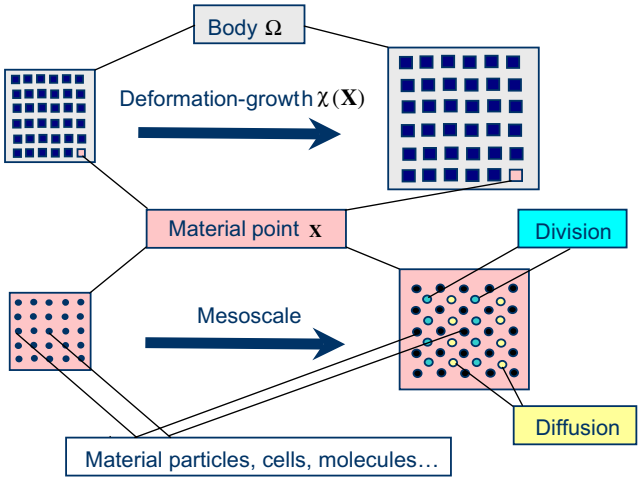

Fig. 1. Multiscale mechanics of growth.

not changing during growth-deformation. Of course, the concept of the material point is purely mathematical. Material points do not exist: they are mathematical abstractions. Material always occupies some volume. In saying 'material point', one means a very small volume. Such small volumes are considered on the mesoscale of the growth-deformation process as shown in Fig. 1. Under 'higher resolution' it can be seen that the material point is a very small physical volume, which in the case of living tissues includes cells, molecules, pores, and various tissue particles. It is crucial that the number of material particles is changing within a material point due to division and diffusion. Therefore, if we could track the behavior of a referential material point we would find the changing mass density within it. The latter means that the referential mass density is changing during deformation-growth: $\rho \neq$ constant, and mass is not conserved. The violation of mass conservation is inherent in open systems exchanging material with their environment.

While the qualitative analysis of the geometry and physics of tissue growth justifies the use of continuum mechanics for an open system, it is insufficient for the development of the particular equations of a macroscopic phenomenological theory. Such development requires some microscopic reasoning in order to motivate the continuum field and constitutive equations. It seems that a reasonable insight into the tissue growth mechanisms can be gained by considering a simple toy-tissue model presented in Fig. 2. The regular initial tissue can be seen on the top of the figure. This is a collection of the regularly packed balls. The balls are interpreted as the tissue elementary components – cells, molecules of the extracellular matrix, etc. The balls are arranged in a regular network for the sake of simplicity and clarity. They can be organized more chaotically – this does not affect the subsequent qualitative analysis. Let us assume now that a new material, i.e., a number of new balls, is supplied pointwise as it is shown on the bottom of Fig. 2. This supply is considered as a result of injection: the tube with the new material is a syringe. Usually, the new material is created in real tissues in a more complicated manner following a chain of biochemical transformations. However, the finally produced new material still appears pointwise from the existing cells. Thus, the injection of the balls is a quite reasonable model of tissue growth. Such a model can be constructed physically, of course. It seems that the latter is not necessary and the toy-tissue model can be easily imagined. The result of such a thought-experiment is represented in the figure and it can be described as follows: (a) the number of the balls in the toy-tissue increases with the supply of the new ones; (b) the new balls are concentrated at the edge of the tube and they do not spread uniformly over the tissue; (c) the new balls cannot be accommodated at the point of their supply – the edge of the tube – they tend to spread over the area at the vicinity of the edge and the packing of the balls gets denser around the edge of the tube; (d) the more balls are injected the less room remains for the new ones; (e) the new balls press the old ones; (f) the new balls tend to expand the area occupied by the tissue when the overall ball rearrangement reaches the tissue surface. These six qualitative features of the toy-tissue microscopic behavior can be translated into the language of the macroscopic theory accordingly: (A) mass of the tissue grows; (B) mass growth is not uniform – the mass density changes from one point to another; (C) there is a diffusion of mass; (D) the diffusion is restricted by the existing tissue structure and its mass density: the denser the tissue is the less material it can accommodate; (E) growth is accompanied by stresses; (F) the expansion of the tissue is volumetric – it is analogous to the thermal expansion of structural materials, such as steel, for example.

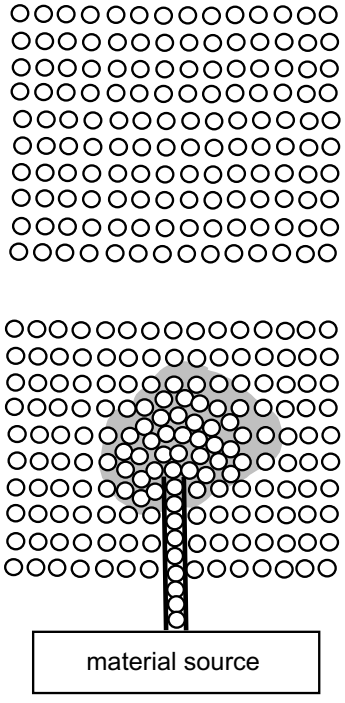

Fig. 2. A microstructural toy-tissue model of material supply.

The first three features (A, B, and C) prompt the form of the quasi-static ($\partial \mathbf{x}/\partial t \approx \mathbf{0}$) mass balance law for growing body Ω:

$$\frac{\partial \rho}{\partial t} = -\mathrm{Div}\,\boldsymbol{\psi} + \xi, \tag{1}$$

where ρ is the referential mass density; $\boldsymbol{\psi}$ is the vector of mass flux per unit reference area; ξ is the current mass supply per unit reference volume; and 'Div' is the divergence operator with respect to the referential coordinates. Indeed, the mass change means the failure of the mass conservation law, which covers most theories of mechanics, and it means the necessity to introduce a full-scale mass balance for an open system. The fact that non-uniform mass growth is related to the diffusion of mass is very important. It means that the mass balance law should include both the volumetric mass source and the surface mass flux. The latter is

missed in many theories of growth. The absence of mass diffusion in the theory leads to a nonphysical conclusion that tissue density can change only at the point of material supply. Mass diffusion should take place in order to accommodate a non-uniform mass supply. Finally, we should mention that some authors do not include mass diffusion in balance equations. Instead of that, they introduce mass diffusion in the constitutive description directly. In this case, the order of the differential equations increases implicitly. The latter is often missed and the necessary additional boundary conditions are lost in computations.

Boundary conditions complete the law of mass balance:

$$\begin{cases} \rho(t=0)=\rho_0 & \text{in } \Omega, \\ \rho=\bar{\rho} & \text{on } \partial\Omega_\rho, \\ \phi=\bar{\phi} & \text{on } \partial\Omega_\phi, \end{cases} \tag{2}$$

where the bar means a given magnitude; $\phi=\boldsymbol{\psi}\cdot\mathbf{n}$ is a current flux per unit reference area; and $\mathbf{n}$ is a unit outward normal to the reference surface $\partial\Omega$.

Momentum balance and corresponding boundary conditions take the traditional form in the case of a quasi-static process (see also Remark 1)

$$\operatorname{Div}\mathbf{P}=\mathbf{0}, \tag{3}$$

$$\mathbf{P}\mathbf{F}^{\mathrm{T}}=\mathbf{F}\mathbf{P}^{\mathrm{T}}, \tag{4}$$

$$\begin{cases} \boldsymbol{\chi}=\bar{\boldsymbol{\chi}} & \text{on } \partial\Omega_\chi, \\ \mathbf{t}=\bar{\mathbf{t}} & \text{on } \partial\Omega_\mathbf{t}, \end{cases} \tag{5}$$

where $\mathbf{P}$ is the first Piola–Kirchhoff stress; $\mathbf{F}=\nabla\boldsymbol{\chi}(\mathbf{X})$ is the deformation gradient; $\boldsymbol{\chi}$ is the current position vector of point $\mathbf{X}$; and $\mathbf{t}=\mathbf{P}\mathbf{n}$ is the surface traction.

The three last features (D, E, and F) of the toy-tissue model motivate the constitutive law. They suggest that the stress–strain relations should be analogous to thermoelasticty where the role of the temperature is played by the mass density: the increase of the mass density results in the volume expansion of the tissue

$$\mathbf{P}=\mathbf{F}(\partial W/\partial\mathbf{E}-(\rho-\rho_0)\boldsymbol{\eta}), \tag{6}$$

where W is a strain potential of a non-growing material; $\mathbf{E}=(\mathbf{F}^{\mathrm{T}}\mathbf{F}-\mathbf{1})/2$ is the Green strain tensor and $\mathbf{1}$ is the identity tensor; and $\boldsymbol{\eta}=\boldsymbol{\eta}^{\mathrm{T}}$ is a symmetric[3] tensor of growth moduli, which are related to the material volume expansion for the increasing mass density. The first term on the right-hand side of Eq. (6) is that of the classical hyperelasticity without growth. The second term is analogous to the small-strain thermoelasticity where the temperature increment is replaced by the density increment. In setting this stress–strain law, we were guided by a microstructural model presented in Fig. 2. It should be noted, however, that the idea of thermoelastic analogy was also considered in Refs. [42,44] in the context of a hypoelastic constitutive model. The first qualitative notion of the analogy between growth and thermal expansion is, probably, due to Skalak [2].

As can be seen in Fig. 2, the mass supply should be resisted by the tissue: the denser the tissue, the less is the new mass accommodation

$$\xi=\omega+f-(\rho-\rho_0)\gamma, \tag{7}$$

where $\omega>0$ is the genetic mass supply, which is analogous to a quasi-static mechanical load for a quasi-static growth process: $\partial\rho/\partial t\approx 0$ (ω is controlled by the tissue itself and its proper determination requires experiments); f is the epigenetic mass supply, which should depend on stress and/or strain measures (its correct expression is a key problem when tissue remodeling is considered); the last term on the right-hand side of Eq. (7) including coefficient of tissue resistance, $\gamma>0$, reflects the resistance of the tissue to accommodate new mass for increasing mass density (roughly speaking, the more new material the less room for it remains).

Finally, we introduce the constitutive equation for mass flux in the simplest Fickean form

$$\boldsymbol{\psi}=-\beta\nabla(\rho-\rho_0), \tag{8}$$

where β is the mass conductivity of the material and ∇ is the gradient operator with respect to the referential coordinates.

The similarity between Eqs. (6) and (8) of growth and analogous equations of (small-strain) thermoelasticity is obvious after replacing the mass density increment by the temperature increment, mass flux by heat flux, mass conductivity by thermal conductivity, etc. In this case, Eq. (6) is nothing but the thermoelastic generalization of Hooke's law, and Eq. (8) is just the Fourier law of heat conduction. The constitutive equation analogous to (7) is usually absent in thermoelasticity because of the lack of volumetric heat sources. The thermoelastic analogy allows for a better understanding of parameters of the growth model. For example, the vector of mass flux is analogous to the vector of heat flux. We feel the heat flow by changing temperature without directly defining what the heat is. The same is true for the mass flow. We 'feel' it by changing mass density without directly defining what it is.

We apply the quasi-static boundary value problem (BVP) described by Eqs. (1)–(8) to the problems of artery and tumor growth in the next two subsections accordingly.

Remark 1. Continuum mechanics frameworks for open systems developed in Refs. [9,15] account for a momentum produced by the new mass supply. The additional momentum is important, indeed, in the case of the missile flight when the missile mass is changing rapidly because the solid fuel is burning out. This is not the case of the very slowly growing tissue. The momentum triggered by the new tissue supply is negligible and it can be ignored in the studies of tissue growth.[4] This is why the linear (3) and angular (4) momentum balance equations enjoy the regular structure.

[3] This symmetry allows for satisfying the angular momentum balance – Eq. (4) – identically.

[4] It is assumed that the newly created material has the same momentum as the existing material, in a local fashion.

2.2. Artery growth

We consider artery growth as a radial growth of an infinite cylinder under the plane strain conditions where all variables depend on the radial coordinate only

$$r = r(R), \quad \theta = \Theta, \quad z = Z, \tag{9}$$

where a point occupying position (R,Θ,Z) in the initial configuration is moving to position (r,θ,z) in the current configuration. Then the deformation gradient takes the form

$$\mathbf{F} = (\partial r/\partial R)\mathbf{k}_r \otimes \mathbf{K}_R + (r/R)\mathbf{k}_\theta \otimes \mathbf{K}_\Theta + \mathbf{k}_z \otimes \mathbf{K}_Z, \tag{10}$$

where $\{\mathbf{K}_R,\mathbf{K}_\Theta,\mathbf{K}_Z\}$ and $\{\mathbf{k}_r,\mathbf{k}_\theta,\mathbf{k}_z\}$ form the orthonormal bases[5] in cylindrical coordinates at the reference and current configurations accordingly.

As a consequence of the deformation assumption we have for the nonzero Green strains

$$2\{E_{RR},E_{\Theta\Theta},E_{\Phi\Phi}\} = \{(\partial r/\partial R)^2 - 1, (r/R)^2 - 1, 0\}. \tag{11}$$

The following nonzero components of the first Piola–Kirchhoff stress tensor

$$\begin{cases} P_{rR} = (ce^{Q}(c_1E_{RR} + c_4E_{\Theta\Theta}) - \eta_{11}(\rho-\rho_0))\partial r/\partial R, \\ P_{\theta\Theta} = (ce^{Q}(c_2E_{\Theta\Theta} + c_4E_{RR}) - \eta_{22}(\rho-\rho_0))r/R, \\ P_{zZ} = (ce^{Q}(c_5E_{\Theta\Theta} + c_6E_{RR}) - \eta_{33}(\rho-\rho_0)) \end{cases} \tag{12}$$

can be obtained for the Fung strain potential (see Remark 2)

$$\begin{aligned} W &= ce^{Q}/2, \\ Q &= c_1E_{11}^2 + c_2E_{22}^2 + c_3E_{33}^2 + 2c_4E_{11}E_{22} + 2c_5E_{33}E_{22} \\ &\quad + 2c_6E_{11}E_{33} \end{aligned} \tag{13}$$

with c the only dimensional elastic parameter and c_i dimensionless.

The nonzero growth moduli are set as follows:

$$\begin{cases} \eta_{11} = c(c_1\alpha_1 + c_4\alpha_2 + c_6\alpha_3), \\ \eta_{22} = c(c_4\alpha_1 + c_2\alpha_2 + c_5\alpha_3), \\ \eta_{33} = c(c_6\alpha_1 + c_5\alpha_2 + c_3\alpha_3), \end{cases} \tag{14}$$

where the coefficients of growth expansion $\alpha = \alpha_1 = \alpha_2 = \alpha_3$ define how much the relative volume changes for the given increment of mass density. These coefficients are analogous to the coefficients of thermal expansion in small-strain thermoelasticity. The specific form of the growth moduli comes from requirement of the thermoelastic analogy for small strains. In this case the constitutive law can be written as $\boldsymbol{\sigma} = \mathbf{C} : (\boldsymbol{\varepsilon} - (\rho-\rho_0)\boldsymbol{\alpha})$, where $\boldsymbol{\sigma} \cong \mathbf{P}$ is the Cauchy stress tensor; $\mathbf{C} = (\partial_{\mathbf{E}}\partial_{\mathbf{E}}W)(\mathbf{E}=\mathbf{0})$ is the linearized tangent stiffness; $\boldsymbol{\varepsilon}$ is the linearized strain tensor; and $\boldsymbol{\alpha} = \mathrm{diag}\{\alpha_1,\alpha_2,\alpha_3\}$ is a diagonal matrix of the growth expansion coefficients. Thus, we have for the growth moduli $\boldsymbol{\eta} = \mathbf{C} : \boldsymbol{\alpha}$ where the components of $\mathbf{C}$ come from the linearization of the Fung potential as it appears in Eq. (14).

Assume also that new material is supplied uniformly, i.e., ω does not depend on position, and genetically only ($f = 0$). In this case,

$$\rho - \rho_0 = \omega/\gamma \tag{15}$$

is a solution of the mass balance equation, where $\partial\rho/\partial t = 0$, and $\phi = \beta\mathbf{n}\cdot\nabla(\rho-\rho_0) = 0$ on the boundary including inner and outer surfaces of the tube.

The equilibrium equation (3) without the body forces takes the form

$$\mathrm{Div}\,\mathbf{P} = \left(\frac{\partial P_{rR}}{\partial R} + \frac{P_{rR} - P_{\theta\Theta}}{R}\right)\mathbf{k}_r = \mathbf{0}, \tag{16}$$

where all components have been defined already.

We will use the Cauchy stress $\boldsymbol{\sigma} = J^{-1}\mathbf{P}\mathbf{F}^{\mathrm{T}}$ for the traction-free boundary conditions

$$\begin{cases} \sigma_{rr}(R=1) = 0, \\ \sigma_{rr}(R=1.3) = 0, \end{cases} \tag{17}$$

where

$$\begin{cases} \sigma_{rr} = J^{-1}\frac{\partial r}{\partial R}P_{rR}, \\ \sigma_{\theta\theta} = J^{-1}\frac{r}{R}P_{\theta\Theta}, \end{cases} \quad J = \frac{r}{R}\frac{\partial r}{\partial R}. \tag{18}$$

After substituting Eqs. (11)–(14) in the equilibrium equation (16) and boundary conditions (17), we have a nonlinear two-point BVP in terms of $r(R)$. The two-point BVP is solved for a number of varying elastic and growth parameters. The solution is obtained by using the shooting method when the initial value problem (IVP) is solved iteratively until fitting the BVP solution. We use Mathematica's IVP solver 'NDSolve' [47].

Remark 2. It is not uncommon that the general requirement of polyconvexity of the strain potential is imposed on the modern constitutive models of soft tissues. Polyconvexity implies the existence of the solution of the statical elasticity problem. It is clear, for example, that the process of rupture of saccular aneurism cannot be described within the framework of elastostatics and the requirement of polyconvexity of the strain potential is physically unreasonable. Actually, none of the existing materials can sustain large deformations in the statical mode. In our opinion, the general requirement of polyconvexity should be replaced by a less restrictive and more physical requirement of the adequate description of material within a given range of stresses and strains by a chosen strain potential. In particular, the experimentally calibrated Fung potential, which is not polyconvex, is adequate for the purpose of our study within the considered range of stresses and strains.

2.3. Tumor growth

Multicell spheroids are usually grown from the existing tumor lines by suspending a few cells in the oxygen- and

[5] $\mathbf{K}_R = (\cos\Theta,\sin\Theta,0)^{\mathrm{T}}$, $\mathbf{K}_\Theta = (-\sin\Theta,\cos\Theta,0)^{\mathrm{T}}$, $\mathbf{K}_Z = (0,0,1)^{\mathrm{T}}$ and $\mathbf{K}_M \otimes \mathbf{K}_N = \mathbf{K}_M\mathbf{K}_N^{\mathrm{T}}$; $\mathbf{k}_r = (\cos\theta,\sin\theta,0)^{\mathrm{T}}$, $\mathbf{k}_\theta = (-\sin\theta,\cos\theta,0)^{\mathrm{T}}$, $\mathbf{k}_z = (0,0,1)^{\mathrm{T}}$ and $\mathbf{k}_m \otimes \mathbf{k}_n = \mathbf{k}_m\mathbf{k}_n^{\mathrm{T}}$.

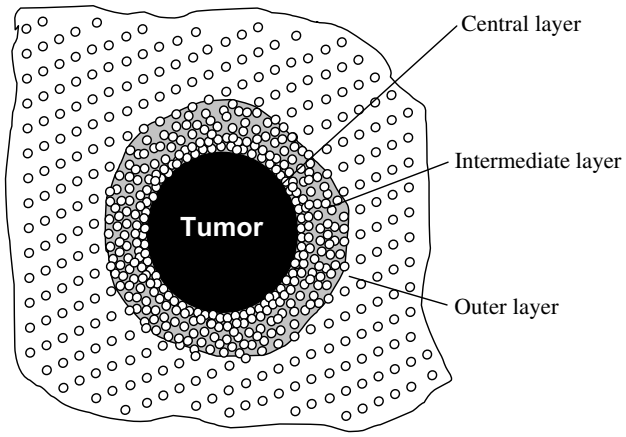

Fig. 3. A microstructural tumor/multicell spheroid model.

nutrient-saturated environment suitable for their growth. Experimental observations [48,49] show that the growing spheroids have a three-layer structure. The outer layer, which is a few cells thick, consists of active and dividing cells. The intermediate layer, which can be three times thicker than the outer layer, consists of non-proliferating cells at rest. The central region consists of the necrotic material composed of the cell debris (Fig. 3).

In the case of the spherically symmetrical growth of the cell spheroid, we restrict deformation to the following one

$$r = r(R), \quad \theta = \Theta, \quad \phi = \Phi, \tag{19}$$

where a point occupying position (R,Θ,Φ) in the initial configuration is moving to position (r,θ,ϕ) in the current configuration. Then the deformation gradient takes the form

$$\mathbf{F} = (\partial r/\partial R)\mathbf{k}_r \otimes \mathbf{K}_R + (r/R)\mathbf{k}_\theta \otimes \mathbf{K}_\Theta + (r/R)\mathbf{k}_\phi \otimes \mathbf{K}_\Phi, \tag{20}$$

where $\{\mathbf{K}_R,\mathbf{K}_\Theta,\mathbf{K}_\Phi\}$ and $\{\mathbf{k}_r,\mathbf{k}_\theta,\mathbf{k}_\phi\}$ form the orthonormal bases[6] in spherical coordinates at the reference and current configurations accordingly; and $\mathbf{k}_m \otimes \mathbf{K}_N = \mathbf{k}_m\mathbf{K}_N^{\mathrm{T}}$.

Then we have for the Green strain

$$2\{E_{RR},E_{\Theta\Theta},E_{\Phi\Phi}\} = \{(\partial r/\partial R)^2 - 1, (r/R)^2 - 1, (r/R)^2 - 1\}. \tag{21}$$

Mass balance (1), momentum balance (3), and constitutive laws (6)–(8) take the following forms accordingly:

$$\partial\psi_R/\partial R + 2\psi_R/R - \xi = 0, \tag{22}$$

$$\partial P_{rR}/\partial R + (2P_{rR} - P_{\theta\Theta} - P_{\phi\Phi})/R = 0, \tag{23}$$

$$\begin{cases} P_{rR} = \partial r/\partial R(\partial W/\partial E_{RR} - (\rho-\rho_0)\eta), \\ P_{\theta\Theta} = r/R(\partial W/\partial E_{\Theta\Theta} - (\rho-\rho_0)\eta), \\ P_{\phi\Phi} = r/R(\partial W/\partial E_{\Phi\Phi} - (\rho-\rho_0)\eta), \end{cases} \tag{24}$$

$$\psi_R = -\beta\partial(\rho-\rho_0)/\partial R, \tag{25}$$

$$\xi = \omega - (\rho-\rho_0)\gamma, \tag{26}$$

[6] $\mathbf{K}_R = (\sin\Theta\cos\Phi, \sin\Theta\sin\Phi, \cos\Theta)^{\mathrm{T}}$, $\mathbf{K}_\Theta = (\cos\Theta\cos\Phi, \cos\Theta\sin\Phi, -\sin\Theta)^{\mathrm{T}}$, $\mathbf{K}_\Phi = (-\sin\Phi, \cos\Phi, 0)^{\mathrm{T}}$; $\mathbf{k}_r = (\sin\theta\cos\phi, \sin\theta\sin\phi, \cos\theta)^{\mathrm{T}}$, $\mathbf{k}_\theta = (\cos\theta\cos\phi, \cos\theta\sin\phi, -\sin\theta)^{\mathrm{T}}$, $\mathbf{k}_\phi = (-\sin\phi, \cos\phi, 0)^{\mathrm{T}}$.

where the remodeling issue is ignored, i.e., $f = 0$; and isotropic growth $\boldsymbol{\eta} = \eta\mathbf{1}$ is assumed.

Boundary conditions (2) and (5) are set as follows:

$$\begin{cases} \rho(R=a) = \omega + \rho_0, \\ \phi(R=\infty) = 0, \end{cases} \tag{27}$$

$$\begin{cases} r(R=a) = a, \\ \sigma_{rr}(R=b) = (r/R)^{-2}P_{rR}(R=b) = \sigma. \end{cases} \tag{28}$$

According to these conditions, it is assumed that the fixed tumor boundary is a source of new mass ω. In addition, it is assumed that mass flux vanishes approaching infinity, i.e., away from the tumor boundary. The condition of infinity is used for the sake of clarity. It will be seen from the obtained results that the density increment decays from the tumor boundary very fast, that infinity is not involved in analysis, and a finite number can replace it. The condition on radial stress away from the tumor boundary is imposed in order to study the effect of the tissue pre-stress on the tumor development.

An isotropic version of the Fung-type material is chosen for numerical simulation. We define the strain potential as follows:

$$\begin{aligned} W &= c_0 e^{Q}/2, \\ Q &= K(\mathrm{tr}\,\mathbf{E})^2 + G(\mathrm{tr}\,\mathbf{E}^2 - (\mathrm{tr}\,\mathbf{E})^2/3) \\ &= c_1(E_{RR}^2 + E_{\Theta\Theta}^2 + E_{\Phi\Phi}^2) \\ &\quad + 2c_2(E_{RR}E_{\Theta\Theta} + E_{RR}E_{\Phi\Phi} + E_{\Phi\Phi}E_{\Theta\Theta}), \end{aligned} \tag{29}$$

where shear strains are ignored for the spherically symmetric deformation; $c_1 = K + 2G/3$ and $c_2 = K - G/3$ are dimensionless parameters; and c_0 is the only dimensional parameter (the dimension of stress).

Differentiating W with respect to strains we get the terms, which appear on the right-hand side of Eq. (24):

$$\begin{cases} \partial W/\partial E_{RR} = c_0 e^{Q}(c_1E_{RR} + c_2E_{\Theta\Theta} + c_2E_{\Phi\Phi}), \\ \partial W/\partial E_{\Theta\Theta} = c_0 e^{Q}(c_1E_{\Theta\Theta} + c_2E_{RR} + c_2E_{\Phi\Phi}), \\ \partial W/\partial E_{\Phi\Phi} = c_0 e^{Q}(c_1E_{\Phi\Phi} + c_2E_{\Theta\Theta} + c_2E_{RR}). \end{cases} \tag{30}$$

Solution of the equation of mass balance (22) with account being taken of boundary conditions (27) provides the following analytical expression for the density increment distribution around the tumor

$$\rho = \omega(R/a)^{-1}\exp[a\tau(1-R/a)] + \rho_0, \tag{31}$$

where $\tau = \sqrt{\gamma/\beta}$ is a normalized tissue resistance parameter (Fig. 4).

Substituting this solution in the equations of momentum balance (23) and imposing boundary conditions (28) it is possible to formulate a nonlinear two-point boundary-value problem for the position function $r(R)$. This problem is solved numerically by using the procedure described in the previous subsection.

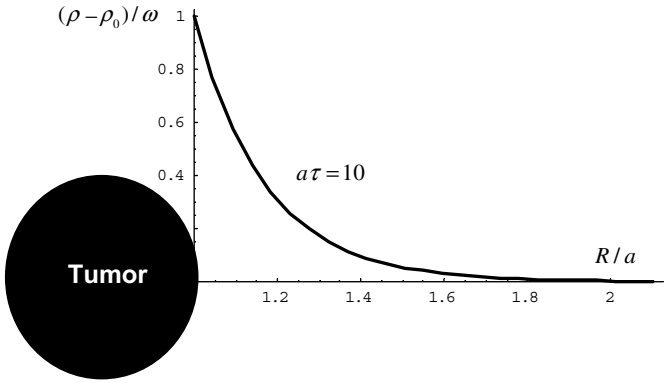

Fig. 4. The exponential decrease of the mass density in the vicinity of tumor surface, Eq. (31).

3. Results

3.1. Artery growth

Radial displacements, radial and circumferential Cauchy stresses (Figs. 5 and 6) were computed for two sets of material parameters:

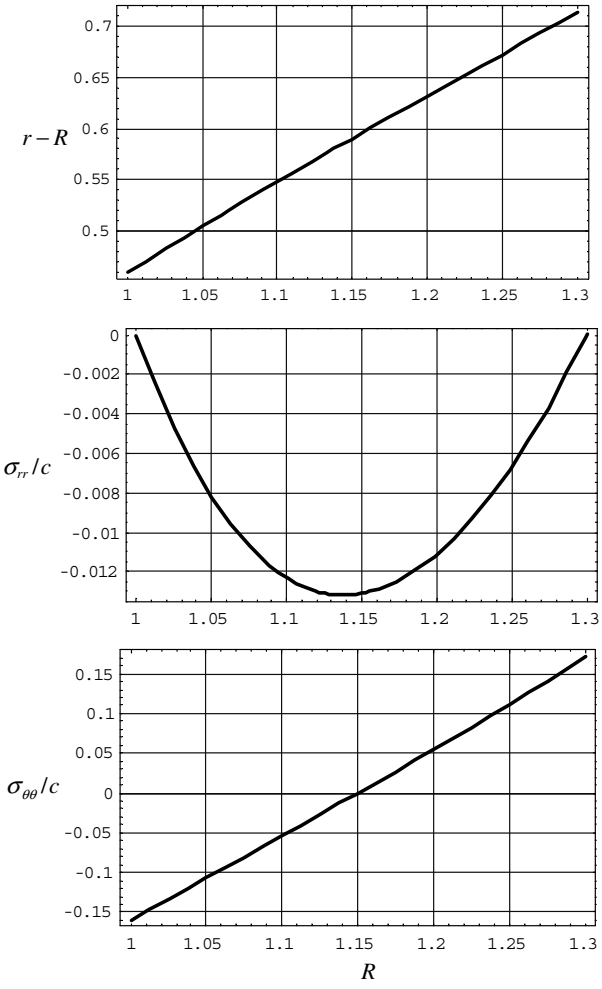

Fig. 5. Radial displacements $(r-R)$ (a); normalized radial stress σ_{rr}/c (b); normalized circumferential stress $\sigma_{\theta\theta}/c$ (c) for $\alpha\omega/\gamma=1$ for free volumetric growth of the cylinder: the first set of material parameters, Eq. (32).

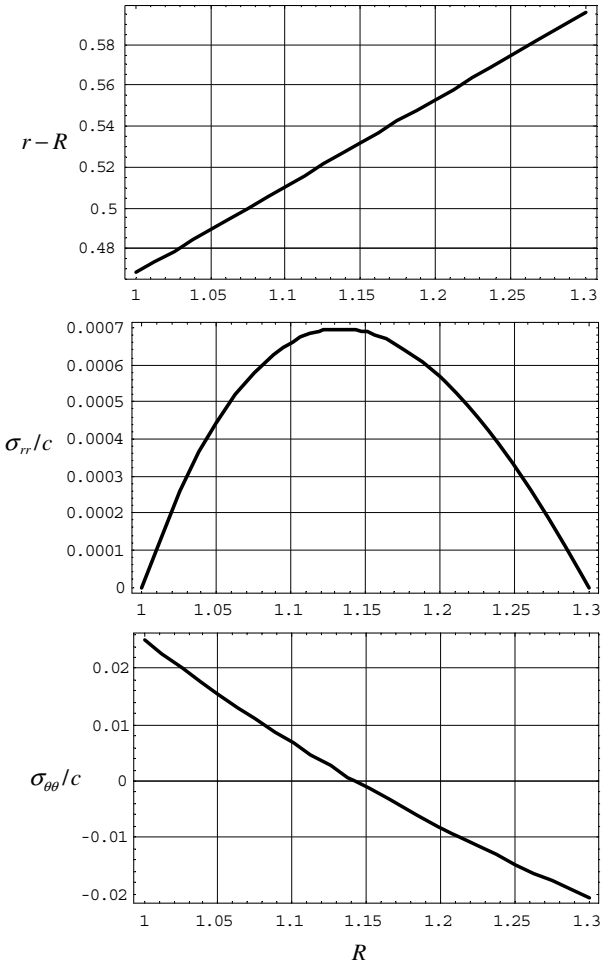

Fig. 6. Radial displacements $(r-R)$ (a); normalized radial stress σ_{rr}/c (b); normalized circumferential stress $\sigma_{\theta\theta}/c$ (c) for $\alpha\omega/\gamma=1$ for free volumetric growth of the cylinder: the second set of material parameters, Eq. (33).

[50]

$$c_1=0.0499;\quad c_2=1.0672;\quad c_3=0.4775;\\ c_4=0.0042;\quad c_5=0.0903;\quad c_6=0.0585. \tag{32}$$

[51]

$$c_1=1.744;\quad c_2=0.619;\quad c_3=0.0405;\\ c_4=0.004;\quad c_5=0.0667;\quad c_6=0.0019. \tag{33}$$

Every set of material parameters was considered with $\alpha\omega/\gamma=1$, which corresponds to the 50% deformation along the radius. Resulting displacements vary almost linearly along the radius (Figs. 5a and 6a). Absolute values of the radial stresses increase towards the mid-surface of the wall (Figs. 5b and 6b), while the absolute values of the circumferential stresses approach zero at the mid-surface and they vary almost linearly along the radius (Figs. 5c and 6c). It should be noted that circumferential stresses are larger than the radial stresses by an order of magnitude in both cases of material parameters. It is interesting that the directions of the stresses are different for the two sets of material parameters. This is, in particular, critical for the circumferential stresses because it means that different bending resul-

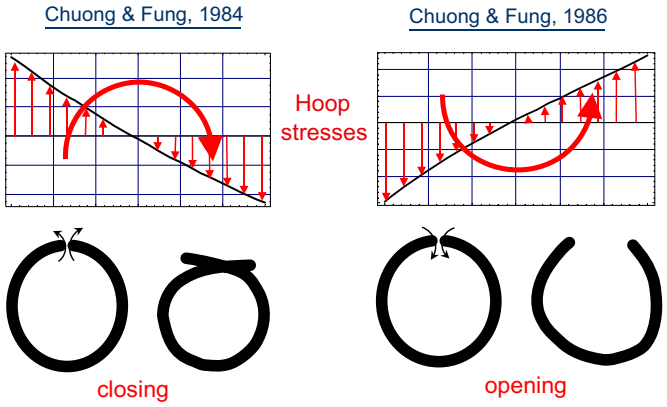

Fig. 7. Bending moments and opening modes for two sets of material parameters.

tants appear in the ring. If the ring is cut radially, then it opens as shown in Fig. 7 (right) for the first set of elastic parameters. A ring with the second set of material parameters behaves differently: it closes (Fig. 7, left) after the cut, i.e., its edges overlap.

3.2. Tumor growth

A wide variety of simulations were carried out based on the described formulation of the growth boundary-value problem in order to reveal the effect of tissue stiffening and stressing on tumor expansion. Two typical sets of results, including displacements and radial and tangent stresses, are presented in Figs. 8 and 9 for the following (unitless) material parameters of the surrounding tissue: $K=1$, $G=3/2$, $\tau=10$, $\eta=1$, $a=1$, $b=5$. In the first set, the elasticity coefficient c_0 was varied from 0.01 to 0.1 and to 1.0 while the material supply was fixed $\omega=1$ and remote stresses were not applied $\sigma=0$ (Fig. 8). In the second set, the remote stress σ was varied from -0.01 to 0.0 and to $+0.01$ while the elasticity coefficient and material supply were constant: $c_0=0.1$; $\omega=1$ (Fig. 9).

The front of the growing tumor does not have a well-defined boundary, instead it is a layer ($1.1<R/a<1.4$) where the mass density increment is decreasing quickly – see Figs. 3 and 4. This front evolves with the supply of new cells. However, its evolution depends on the stiffness of the hosting tissue, as follows from Fig. 8 at the top. The maximum displacements $(r-R)$ correspond to the tumor front and they decay away from the tumor. It is crucial that the peak displacements at the tumor front are essentially different for various tissue stiffnesses. For a 'soft' tissue with $c_0=0.01$, the tumor front advances up to 25% of the initial tumor radius; for an 'intermediate' tissue with $c_0=0.1$, the tumor front advances up to 12% of the initial tumor radius; and for a 'hard' tissue with $c_0=1.0$, the tumor front advances up to 3% of the initial tumor radius.

Radial σ_{rr} and tangent $\sigma_{\theta\theta}=\sigma_{\phi\phi}$ stresses generated in the area of tumor growth also change for the varying tissue stiffness – Fig. 8 mid and bottom accordingly. The

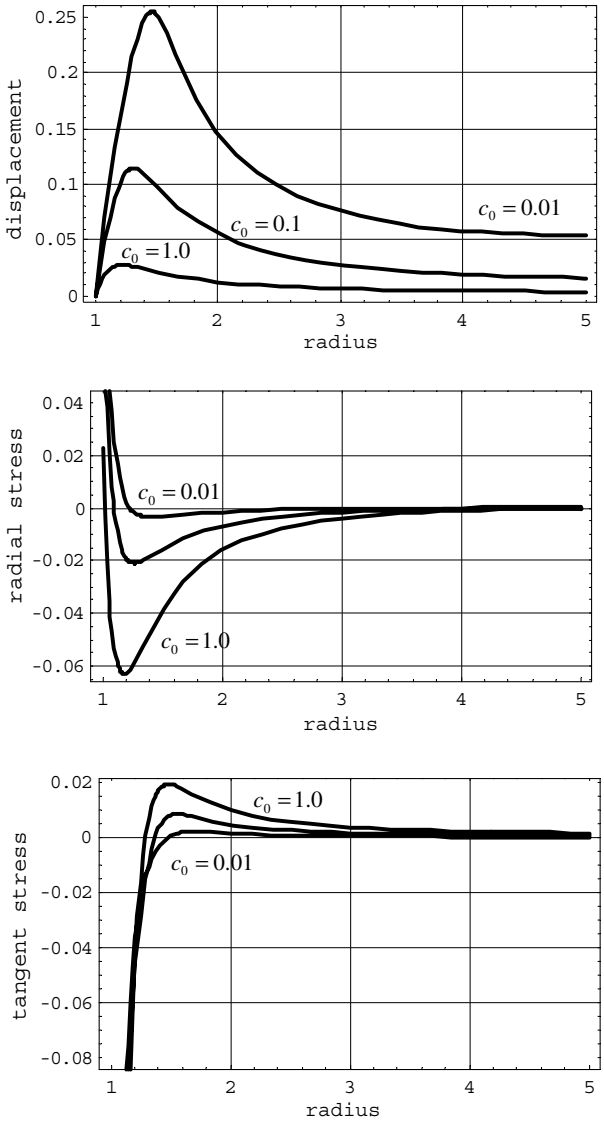

Fig. 8. Displacements (top), radial stresses (middle), and tangent stresses (bottom) around the tumor under varying tissue stiffness $c_0=0.01;0.1;1.0$.

maximum absolute values of these stresses occur at the surface of material supply where the density increment is most significant. These magnitudes are not seen in the figure and we give them explicitly

$$\sigma_{rr}(R=a)=\begin{cases}0.13 & (c_0=0.01),\\ 0.09 & (c_0=0.10),\\ 0.02 & (c_0=1.00),\end{cases}$$

$$\sigma_{\theta\theta}(R=a)=\begin{cases}-0.38 & (c_0=0.01),\\ -0.44 & (c_0=0.10),\\ -0.56 & (c_0=1.00).\end{cases}$$

Evidently, compressive tangent stresses dominate the area of tumor growth and they increase with the increasing stiffness of the hosting tissue.

The front of the growing tumor is weakly affected by the varying remote stresses while the displacements outside the growing tumor are very sensitive to these stresses – Fig. 9

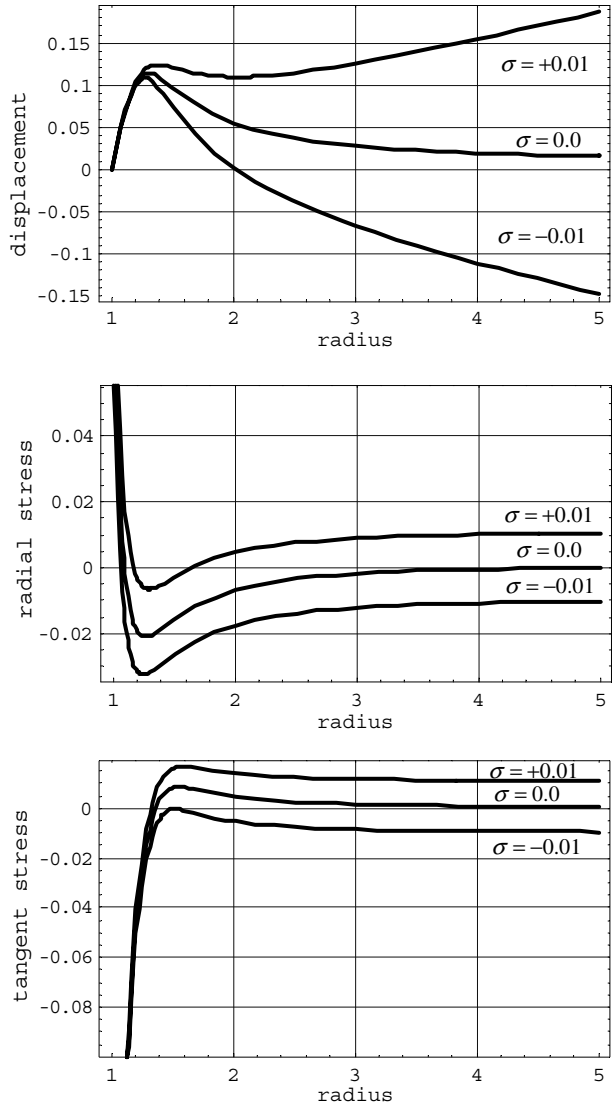

Fig. 9. Displacements (top), radial stresses (middle), and tangent stresses (bottom) around the tumor under varying remote stress $\sigma = -0.01; 0.0; +0.01$.

top. Indeed, the peak displacement at the tumor front does not change much in tension, compression, or the neutral state. In contrast, the displacements at the distance of $R = 3a$ are essentially different and the radial material fibers can shorten or lengthen depending on the remote compression or tension accordingly. The radial and tangent stresses away from the tumor are shifted with respect to each other in correspondence with the remote stresses. The magnitudes of the stresses at the surface of material supply are as follows:

$$\sigma_{rr}(R=a) = \begin{cases} 0.11 & (\sigma = +0.01), \\ 0.09 & (\sigma = 0.00), \\ 0.07 & (\sigma = -0.01), \end{cases}$$

$$\sigma_{\theta\theta}(R=a) = \begin{cases} -0.43 & (\sigma = +0.01), \\ -0.44 & (\sigma = 0.00), \\ -0.44 & (\sigma = -0.01). \end{cases}$$

4. Discussion

4.1. Artery growth

A simple phenomenological theory of tissue growth has been used in the present work for qualitatively explaining the phenomenon of residual stresses in arteries. Material anisotropy was included in the theoretical setting in accordance with the experimental data. The theory was applied to the problem of free and uniform radial growth of a cylindrical blood vessel. Displacement and stress fields were computed for the experimentally obtained values of the elasticity parameters. The computations give evidence of the appearance of the circumferential stresses resulting in the bending moments, which provide the compatibility of the grown arterial cross-section. The radial cut of the arterial ring will lead to the release of the bending moments and opening or closing of the ring as it is observed in experiments.

It is important that the circumferential stresses, which are accumulated into the residual stresses during the long-term growth, appear due to anisotropy. These stresses would not appear in the 'isotropic artery'. The latter suggests the interpretation of the arterial anisotropy as a constraint imposed on the volumetric growth. It is interesting that this conclusion is novel as compared to the traditional point of view that the material inhomogeneity and differential growth are the main sources of the residual stresses [4,52]. It is very likely that the material anisotropy is a complementary factor to the material inhomogeneity and differential growth in causing the residual stresses. In principle, the considered theory allows for including the material inhomogeneity and differential growth in analysis. Unfortunately, there is no clear enough experimental data to do so yet.

It is equally important that depending on the specific values of the elasticity moduli both ring closing or opening may take place after the radial cut as shown in Fig. 7. Both these scenarios are in a qualitative agreement with the experimental data [53–57].

It should not be missed that also radial stresses appear in the considered arterial growth. The magnitude of these stresses is of lower order as compared to circumferential stresses. Nonetheless, the radial stresses can play a role in forming the global residual stresses. Particularly, the radial stresses are a good candidate for the explanation of Vossoughi experiments [58]. These authors cut the opened artery ring along the midline and found that the inside segment opened more while the outside segment closed more. Probably, this happened because the radial residual stresses had been relieved partially.

Finally, it is worth emphasizing that we gave a qualitative explanation of the residual stresses in arteries. In order to estimate the residual stresses quantitatively *in vivo* experiments are necessary. The existing attempts of the quantitative estimate of the residual stresses in arteries based on the *in vitro* ring-cutting techniques may not be reliable. The problem is that every cut leads to a redistribution of residual stresses. This redistribution of stresses starts from

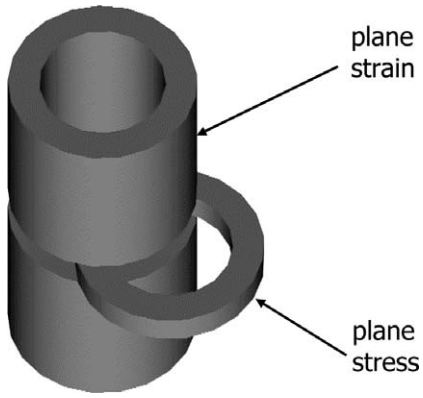

Fig. 10. Redistribution of stresses as a result of the ring cutting.

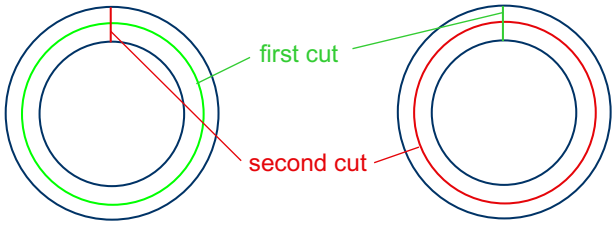

Fig. 11. A suggested experiment for the demonstration of the stress redistribution under cutting.

the very first cut when a ring is taken from the artery (Fig. 10). Indeed, such a ring is approximately under the plane strain state before the cut. However, after the cut the state of the ring is closer to the plane stress. Thus, extracting the ring from the artery we cause a new distribution of stresses in it. This same happens after all subsequent cuts. Actually, every subsequent cut relieves stresses in the previous configuration and not in the initial one. In order to illustrate this point we suggest the following experiment – Fig. 11. Let two neighbor rings be cut from an artery in such place along the artery that it is reasonable to assume that the residual stresses are the same in both rings. These rings are further cut radially and circumferentially, i.e., along the midline. It is crucial, however, that the order of cutting is different for the different rings. One ring should be cut first radially and then circumferentially, while the other ring should be cut first circumferentially and then the two obtained thinner rings should be cut radially separately. Both initial rings are finally split into two open segments. This is done, however, in the different sequences of cuts. The final shape of the segments should be different in both cases because the order of cutting *does* matter for *large deformations* where the superposition principle is not valid. Indeed, the cutting is equivalent to applying tractions on the cut surfaces to make these surfaces traction-free. In the case of large deformations, the order of application of the external forces is crucial. The difference in the experimentally cut segments should be visible if the residual radial stresses are comparable in the magnitude with the residual circumferential stresses. The expected results of the described experiment could clearly illustrate insufficiency of the artery-cutting experiments for estimating the magnitudes of the residual stresses. It seems that the artery-cutting experiments can only be useful for the qualitative comparison purposes and not for the quantitative estimates of the residual stresses: the more artery is cut, the less information can be gained about its residual stresses.

4.2. Tumor growth

Experimental observation of the inhibited tumor growth under stiffening of the hosting tissue has been explained theoretically in the present work. For this purpose, a simple microstructural model of tumor growth was considered. This model was used as a basis for the subsequent development of a continuum solid mechanics theory of tumor growth. In addition to the classical momentum balance laws, the theory includes a full-scale mass balance law, i.e., volumetric mass supply and mass diffusion. The latter allows for an average description of the cell proliferation out of the tumor. The diffusive term, which is missed in most modern theories of tissue growth, is critical for a physically reasonable description of the tumor expansion. Besides the balance law, the microstructural model also prompts the form of constitutive equations. In the case of small strains, these equations are analogous to thermoelasticity where the temperature increment is replaced by mass density increment, and the growth process is considered analogous to a thermal expansion. A problem of spherically symmetric growth of a pre-existing tumor was considered within the framework of the developed theory. It was assumed that material surrounding the tumor is Fung-type isotropic. Such material is characteristic of living tissues, which exhibit exponential stiffening behavior because of the straightening of collagens and other long molecules comprising the material matrix.

Qualitatively, the results of numerical simulations can be summarized as follows:

(I) In perfect correspondence with histological examination, computer modeling revealed that active growth is restricted to a thin shell at the periphery of the tumor.
(II) Growth is accompanied by stressing and compressive tangent stresses dominate, which may potentially lead to the tumor patterning [59].
(III) Consistent with experiments on multicellular tumor spheroids, computer modeling shows that stiffening of the hosting tissue inhibits growth.
(IV) Moderate remote stressing of the hosting tissue should not essentially affect tumor development.

The fact that tissue stiffening inhibits growth prompts an idea to reinforce the real tissue surrounding the actively growing tumor by injecting small solid particles. In this way it is possible to significantly stiffen the tissue and encapsulate the tumor preventing from its expansion.

The explanation of the inhibited tumor growth given in the present work includes various assumptions, i.e., spherical symmetry, quasi-equilibrium state, material isotropy, boundary conditions on infinity, etc. These assumptions seem to be reasonable for a qualitative explanation of the observed phenomenon. It is crucial that the proposed theory does not rely upon any kind of internal variables, which are not accessible in experiments. If the properties of a real tissue, as well as the characteristics of the tumor are known, then the theory can be calibrated and it can be used for quantitative predictions of the tumor development. The latter may be important in tumor treatment and preoperative planning.

References

[1] Hsu FH. The influence of mechanical loads on the form of a growing elastic body. J Biomech 1968;1:303–11.

[2] Skalak R. Growth as a finite displacement field. In: Carlson DE, Shield RT, editors. Proceedings of the IUTAM symposium on finite elasticity. Dordrecht: Martinus Nijhoff Publishers; 1982. p. 347–55.

[3] Skalak R, Dasgupta G, Moss M, Otten E, Dullimeijer P, Villeman H. Analytical description of growth. J Theor Biol 1982;94:555–77.

[4] Fung YC. Biomechanics: motion flow, stress, and growth. New York: Springer; 1990.

[5] Drozdov AD. Viscoelastic structures: mechanics of growth and aging. San Diego (CA): Academic Press; 1998.

[6] Rodriguez EK, Hoger A, McCulloch AD. Stress-dependent finite growth in soft elastic tissues. J Biomech 1994;27:455–67.

[7] Taber LA. Biomechanics of growth, remodeling, and morphogenesis. Appl Mech Rev 1995;48:487–545.

[8] Chen YC, Hoger A. Constitutive functions of elastic materials in finite growth and deformation. J Elast 2000;59:175–93.

[9] Epstein M, Maugin G. Thermomechanics of volumetric growth in uniform bodies. Int J Plast 2000;16:951–78.

[10] Rachev A. A model of arterial adaptation to alterations in blood flow. J Elast 2000;61:83–111.

[11] Taber LA, Perucchio R. Modeling heart development. J Elast 2000;61:165–97.

[12] Kuhn S, Hauger W. A theory of adaptive growth of biological materials. Arch Appl Mech 2000;70:183–92.

[13] Klisch SM, Van Dyke TJ, Hoger A. A theory of volumetric growth for compressible elastic biological materials. Math Mech Solids 2001;6:551–75.

[14] Humphrey JD. Cardiovascular solid mechanics. New York: Springer; 2002.

[15] Kuhl E, Steinman P. Mass- and volume-specific views on thermodynamics for open systems. Proc R Soc London A 2003;459:2547–68.

[16] Garikipati K, Arruda EM, Grosh K, Narayanan H, Calve S. A continuum treatment of growth in soft biological tissues: the coupling of mass transport and mechanics. J Mech Phys Solids 2004;52:1595–625.

[17] Menzel A. Modeling of anisotropic growth in biological tissues. Biomech Model Mechanobiol 2005;3:147–71.

[18] Klisch SM, Hoger A. Volumetric growth of thermoelastic materials and mixtures. Math Mech Solids 2003;8:337–402.

[19] Klisch SM, Chen SS, Sah RL, Hoger A. A growth mixture theory for cartilage with application to growth-related experiments on cartilage explants. J Biomech Eng 2003;125:169–79.

[20] Klisch SM, Sah RL, Hoger A. A cartilage growth mixture model for infinitesimal strains: solutions of boundary-value problems related to in vitro growth experiments. Biomech Model Mechanobiol 2005;3:209–23.

[21] Volokh KY. A simple phenomenological theory of tissue growth. Mol Cell Biomech 2004;1:147–60.

[22] Volokh KY, Lev Y. Growth, anisotropy, and residual stresses in arteries. Mol Cell Biomech 2005;2:27–40.

[23] Guillou A, Ogden RW. Growth in soft biological tissue and residual stress development. In: Holzapfel GA, Ogden RW, editors. Mechanics of biological tissue. Proceedings of the IUTAM symposium, Graz, Austria, June–July 2004. Springer; 2006. p. 47–62.

[24] Winsor CP. The Gompertz curve as a growth curve. PNAS 1932;18:1–7.

[25] Gompertz G. On the nature of the function expressive of the law of human mortality, and on the new mode of determining the value of life contingencies. Philos Trans Royal Soc London 1825;115:513–85.

[26] Helmlinger G, Netti PA, Lichtenbeld HC, Melder RJ, Jain RK. Solid stress inhibits the growth of multicellular tumor spheroids. Nature Biotech 1997;15:778–83.

[27] Araujo RP, McElwain DLS. A history of the study of solid tumor growth: the contribution of mathematical modeling. Bull Math Biol 2004;66:1039–91.

[28] McElwain DLS, Pettet GJ. Cell migration in multicell spheroids: swimming against the tide. Bull Math Biol 1993;55:655–74.

[29] Adam JA. A mathematical model of tumor growth. II Effects of geometry and spatial uniformity on stability. Math Biosci 1987;86:183–211.

[30] Byrne HM, Chaplain MAJ. Mathematical models for tumor angiogenesis: numerical simulations and nonlinear wave solutions. Bull Math Biol 1995;57:461–86.

[31] Byrne HM, Chaplain MAJ. Modeling the role of cell–cell adhesion in the growth and development of carcinomas. Math Comp Model 1996;24:1–17.

[32] Greenspan HP. Models for the growth of a solid tumor by diffusion. Stud Appl Math 1972;52:317–40.

[33] McElwain DLS, Morris LE. Apoptosis as a volume loss mechanism in mathematical models of solid tumor growth. Math Biosci 1978;39:147–57.

[34] Ward JP, King JR. Mathematical modeling of avascular tumor growth. IMA J Math Appl Med Biol 1997;14:39–69.

[35] Anderson ARA, Chaplain MAJ. Continuous and discrete mathematical models of tumor-induced angiogenesis. Bull Math Biol 1998;60:857–99.

[36] Orme ME, Chaplain MAJ. Two-dimensional models of tumor angiogenesis and anti-angiogenesis strategies. IMA J Math Appl Med Biol 1997;14:189–205.

[37] Sleeman BD, Nimmo HR. Fluid transport in vascularized tumors and metastasis. IMA J Math Appl Med Biol 1997;15:53–63.

[38] Landman KA, Please CP. Tumor dynamics and necrosis: surface tension and stability. IMA J Math Appl Med Biol 2001;18:131–58.

[39] Please CP, Pettet GJ, McElwain DLS. A new approach to modeling the formation of necrotic regions in tumors. Appl Math Lett 1998;11:89–94.

[40] Please CP, Pettet GJ, McElwain DLS. Avascular tumor dynamics and necrosis. Math Mod Met Appl Sci 1999;9:569–79.

[41] Chen CY, Byrne HM, King JR. The influence of growth-induced stress from the surrounding medium on the development of multicell spheroids. Math Biol 2001;43:191–200.

[42] Jones AF, Byrne HM, Gibson JS, Dold JW. A mathematical model of stress induced during avascular tumor growth. Math Biol 2000;40:473–99.

[43] Lubkin SR, Jackson T. Multiphase mechanics of capsule formation in tumors. J Biomech Eng 2002;124:237–43.

[44] Roose T, Netti PA, Munn LL, Boucher Y, Jain RK. Solid stress generated by spheroid growth estimated using a linear poroelasticity model. Microvasc Res 2003;66:204–12.

[45] Ambrosi D, Mollica F. On the mechanics of a growing tumor. Int J Eng Sci 2002;40:1297–316.

[46] Ambrosi D, Mollica F. The role of stress in the growth of a multicell spheroid. J Math Biol 2004;48:477–99.

[47] Wolfram S. The Mathematica Book. 5th ed. Champaign (IL): Wolfram Media; 2003.

[48] Acker H, Carlsson J, Durand R, Sutherland RM, editors. Spheroids in cancer research. Berlin: Springer-Verlag; 1984.

[49] Sutherland RM. Cell and environment interactions in tumor microregions: the multicell spheroid model. Science 1988;240:177–84.
[50] Chuong CJ, Fung YC. On residual stress in arteries. J Biomech Eng 1986;108:189–92.
[51] Chuong CJ, Fung YC. Compressibility and constitutive relation of arterial wall in radial experiments. J Biomech 1984;17:35–40.
[52] Fung YC. What are the residual stresses doing in our blood vessels. Ann Biomed Eng 1991;19:237–49.
[53] Fung YC. Biodynamics: circulation. New York: Springer; 1984.
[54] Fung YC. Biomechanics: mechanical properties of living tissues. 2nd ed. New York: Springer; 1993.
[55] Rachev A, Greenwald SE. Residual strains in conduit arteries. J Biomech 2003;36:661–70.
[56] Saini A, Berry C, Greenwald SE. Effect of age and stress on residual stress in aorta. J Vasc Res 1995;32:398–405.
[57] Vaishnav RN, Vossoughi J. Residual stress and strain in aortic segments. J Biomech 1987;20:235–9.
[58] Vossoughi J, Hedjazi Z, Borris FS. Intimal residual stress and strain in large arteries. In: Langrana NA et al., editors. Proceedings of the summer bioengineering conference. New York: ASME; 1993. p. 434–7.
[59] Volokh KY. Tissue morphogenesis: a surface buckling mechanism. Int J Devel Biol 2006;50:359–65.